

1
2
3 **SUPPORTING INFORMATION**
4

5 **Metal Cations as Inorganic Structure-Directing Agents during the**
6 **Synthesis of Phillipsite and Tobermorite**
7

8 Juan Carlos Vega-Vila^{1,2}, Advait Holkar², Ross A. Arnold^{1,2,3}, Dale Prentice^{1,3}, Shiqi Dong^{1,3},
9 Longwen Tang³, Erika Callagon La Plante⁴, Kirk Ellison⁵, Aditya Kumar⁶, Mathieu Bauchy³,
10 Samanvaya Srivastava^{1,2,8*}, Gaurav Sant^{1,3,7,8}, Dante Simonetti^{1,2*}
11

12 ¹ Institute for Carbon Management (ICM), University of California, Los Angeles, CA, USA

13 ² Department of Chemical and Biomolecular Engineering, University of California, Los Angeles,
14 CA, USA

15 ³ Department of Civil and Environmental Engineering, University of California, Los Angeles,
16 CA, USA

17 ⁴ Department of Materials Science and Engineering, University of Texas at Arlington, TX, USA

18 ⁵ Electric Power Research Institute (EPRI), Charlotte, NC, USA

19 ⁶ Department of Materials Science and Engineering, Missouri University of Science and
20 Technology, Rolla, MO, USA

21 ⁷ Department of Materials Science and Engineering, University of California, Los Angeles, CA,
22 USA

23 ⁸ California Nanosystems Institute (CNSI), University of California, Los Angeles, CA, USA
24

25 * Corresponding author. E-mail: dasimonetti@ucla.edu; samsri@ucla.edu
26
27
28
29

30 *Corresponding author. E-mail: dasimonetti@ucla.edu
31

32 **S.1. Synthesis of silicate hydrates at varied charge ratios.**

33 Table S.1 encloses the molar compositions of the synthesis precursors for all samples
 34 discussed in the main text. The alkaline content (OH/Si) was kept constant in experiments
 35 performed within the same series (e.g., crystallized at the same temperature) to minimize
 36 morphological and topological differences associated with changes in pH during hydrothermal
 37 treatments.

38 **Table S.1.** Molar composition of synthesis precursors in growth solutions prior to hydrothermal
 39 treatments at 373 and 393 K.

| Sample | C.R. ^a | Na | K | Ca | Al | Si | H ₂ O | OH/Si |
|----------------------------|-------------------|------|------|------|------|----|------------------|-------|
| PHI-TOB-373-0 ^b | 0.00 | 1.41 | 0.39 | - | 0.11 | 1 | 270.27 | 1.47 |
| PHI-TOB-373-0 | 0.00 | 1.41 | 0.39 | - | 0.11 | 1 | 17.59 | 1.47 |
| PHI-TOB-373-0.25 | 0.25 | 1.06 | 0.29 | 0.22 | 0.11 | 1 | 17.59 | 2.66 |
| PHI-TOB-373-0.50 | 0.50 | 0.70 | 0.19 | 0.45 | 0.11 | 1 | 17.59 | 2.63 |
| PHI-TOB-373-0.75 | 0.75 | 0.35 | 0.10 | 0.67 | 0.11 | 1 | 17.59 | 2.61 |
| PHI-TOB-373-1.00 | 1.00 | - | - | 0.90 | 0.11 | 1 | 17.59 | 2.58 |
| PHI-TOB-393-0.00 | 0.00 | 0.99 | 0.51 | - | 0.05 | 1 | 18 | 2.13 |
| PHI-TOB-393-0.30 | 0.30 | 0.70 | 0.36 | 0.23 | 0.05 | 1 | 18 | 2.10 |
| PHI-TOB-393-0.50 | 0.50 | 0.50 | 0.26 | 0.38 | 0.05 | 1 | 18 | 2.07 |
| PHI-TOB-393-0.80 | 0.80 | 0.20 | 0.10 | 0.60 | 0.05 | 1 | 18 | 2.04 |
| PHI-TOB-393-1.00 | 1.00 | - | - | 0.83 | - | 1 | 18 | 2.02 |

40 ^a Fraction of calcium with respect to the total metal cations in the synthesis gel (i.e., $(2 \times \text{Ca}^{2+})/(\text{K}^{+} + \text{Na}^{+} + (2 \times$
 41 $\text{Ca}^{2+}))$).

42 ^b Synthesis performed at varied water content to lower the total silicon concentration to 0.2 M.

43
 44

45 **S.2. Characterization of physicochemical properties of phillipsite and tobermorite samples.**

46 N_2 adsorption isotherms (77 K) are compiled in Figures S.1–S.6 on all phillipsite and
47 tobermorite samples. Samples are referred to as PHI-TOB-X-Y, where X is the temperature of the
48 hydrothermal treatment and Y is the charge ratio (fraction of the cationic content provided by
49 calcium, $Ca/(K + Na + Ca)$). Micropore volumes ($cm^3 g^{-1}$) were determined from semi-log
50 derivative analysis of the isotherm ($\partial(V_{ads}/g)/\partial(\log(P/P_0))$ vs. $\log(P/P_0)$), where the first maximum
51 represents the micropore filling transition and the subsequent minimum represents the end of
52 micropore filling. We note that the micropore volumes (Fig. 2, main text) of samples with mixed
53 phillipsite and tobermorite phases are within the range of the pure phases, highlighting the ability
54 of the single-step synthesis protocols reported here to crystallize materials with structural
55 characteristics of both, phillipsite zeolites and tobermorite silicate hydrates. The hysteresis
56 observed in the desorption portion of the isotherms indicate the presence of mesoporous cavities
57 within PHI-TOB samples.

58

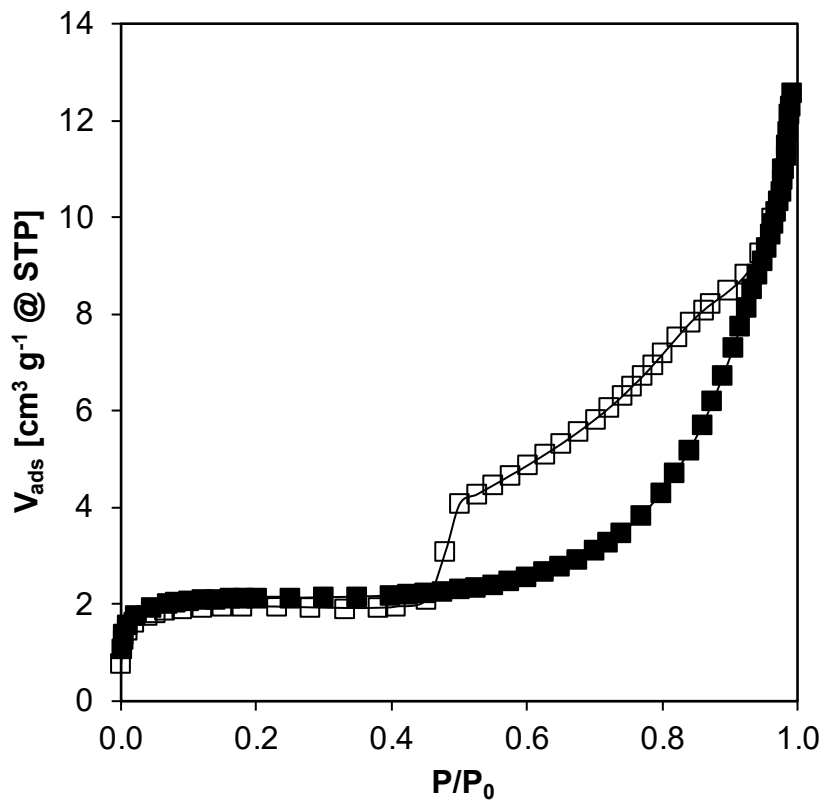


Figure S.1. N₂ adsorption (■) and desorption (□) isotherms (77 K) of PHI-TOB-373-0.

59

60

61

62

63

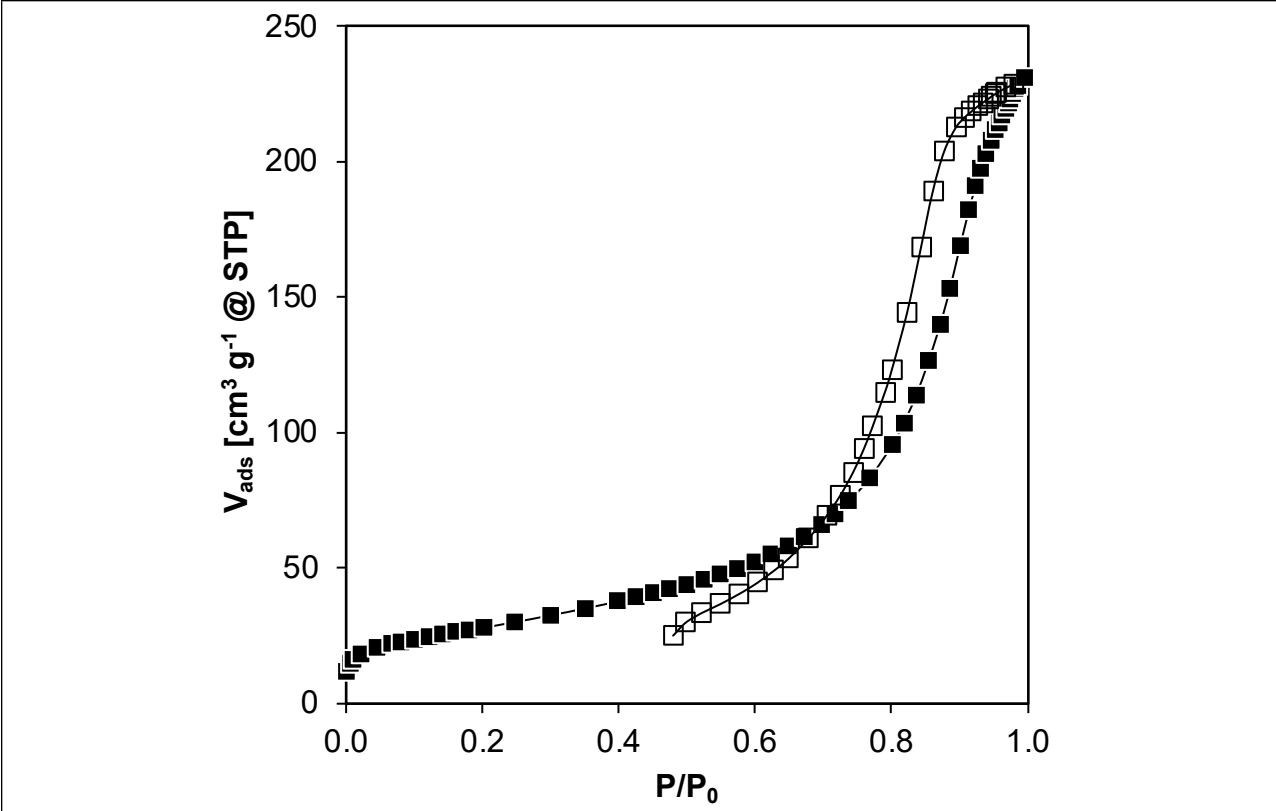


Figure S.2. N₂ adsorption (■) and desorption (□) isotherms (77 K) of PHI-TOB-373-0.25.

64
65

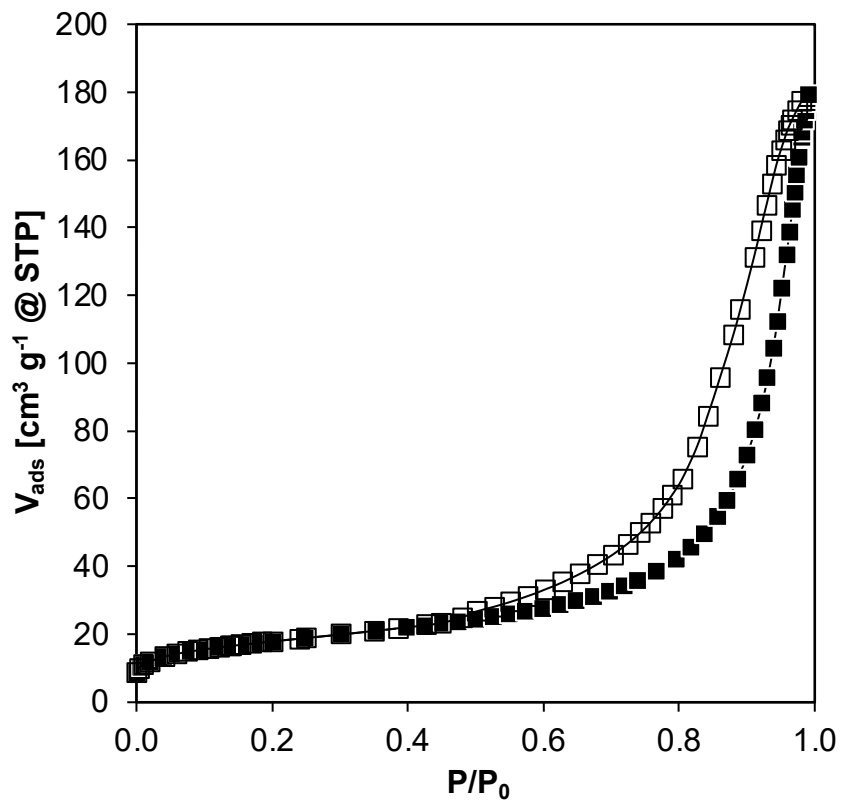


Figure S.3. N₂ adsorption (■) and desorption (□) isotherms (77 K) of PHI-TOB-373-0.50.

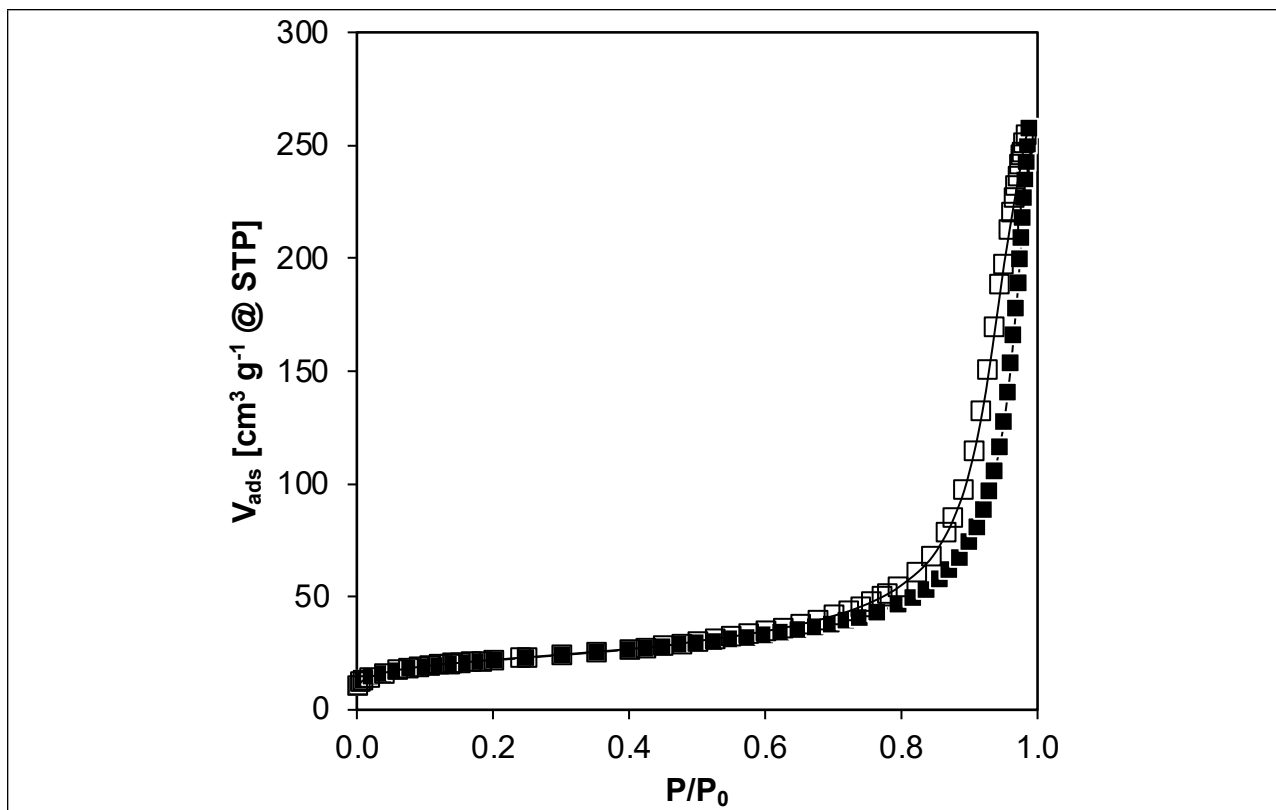


Figure S.4. N₂ adsorption (■) and desorption (□) isotherms (77 K) of PHI-TOB-373-0.75.

68
69

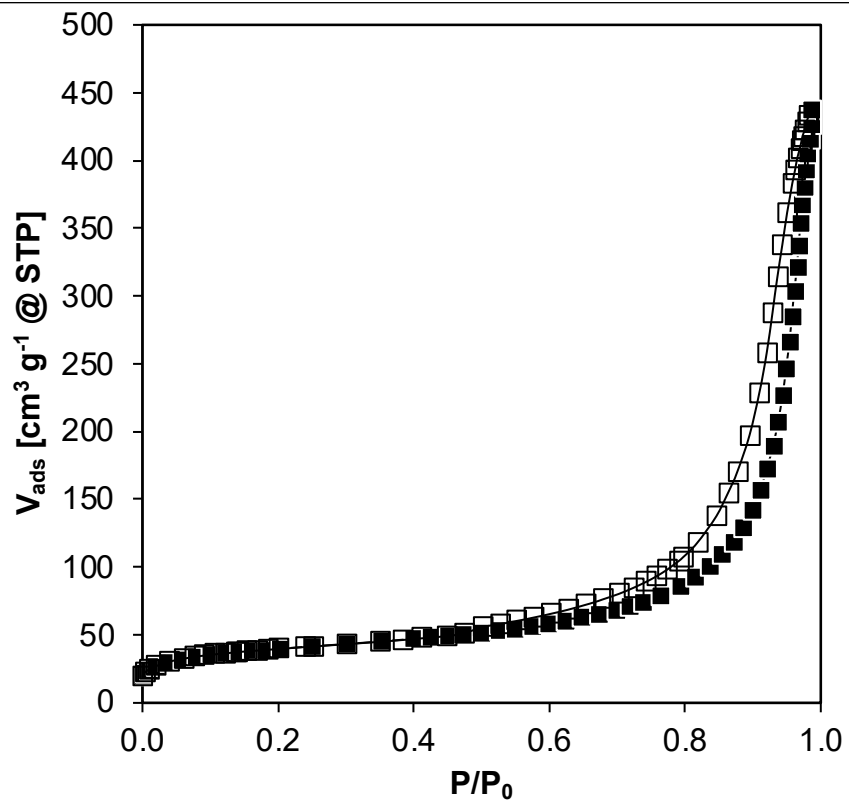


Figure S.5. N₂ adsorption (■) and desorption (□) isotherms (77 K) of PHI-TOB-393-0.80.

70
71
72

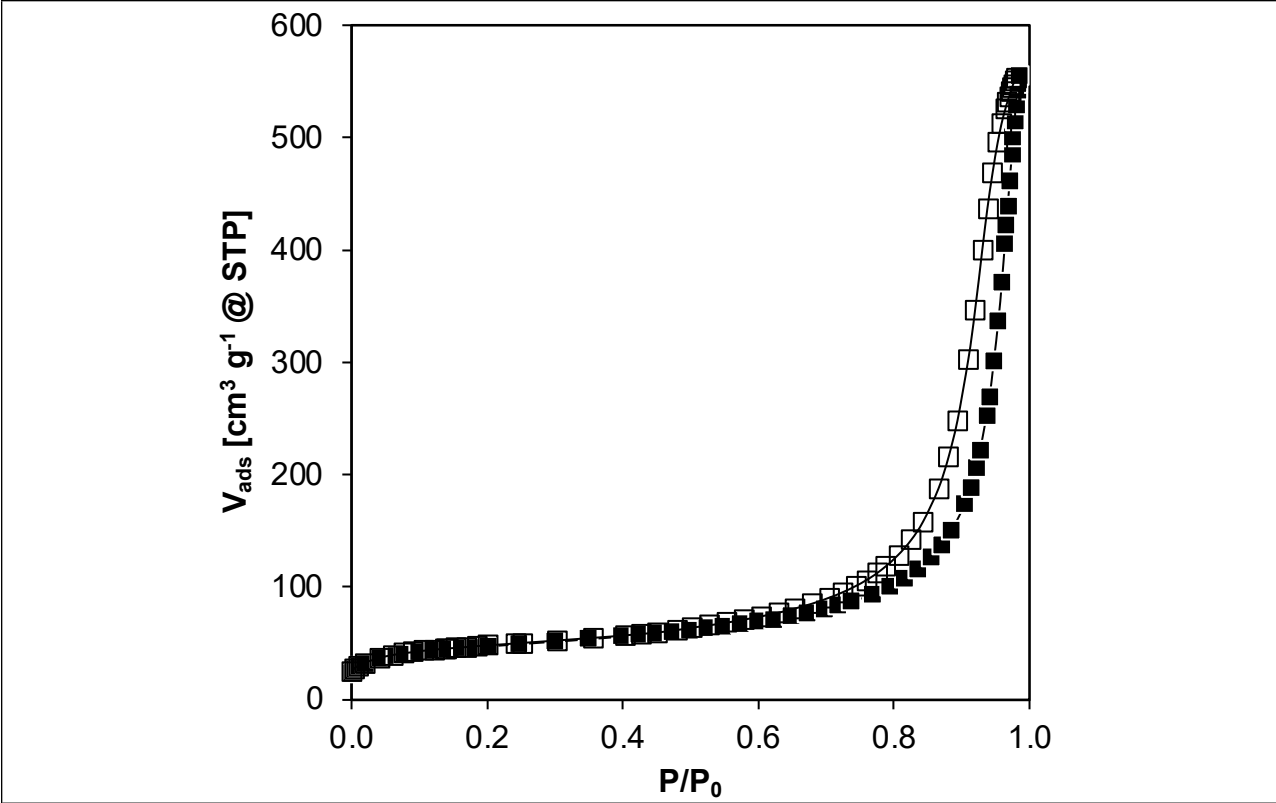


Figure S.6. N₂ adsorption (■) and desorption (□) isotherms (77 K) of PHI-TOB-393-1.

75 **S.3. Morphological signatures of phillipsite zeolites and tobermorite silicate hydrates.**

76 Transmission electron microscope (TEM) images were taken on PHI-TOB-373-0 (Figure
77 S.7) and PHI-TOB-393-1 (Figure S.8). Phillipsite samples (Figure S.7, PHI-TOB-373-0) show
78 planar surfaces that agglomerate to form thick plates, in accordance with their typical prism-like
79 to lath-like morphology with “cracking” along cleavage surfaces.¹ Defined planar surfaces, as well
80 as agglomeration of needle-like crystals, however, are observed for tobermorite samples (Figure
81 S.8). These observation corroborate the presence of tobermorite silicate hydrates as they
82 traditionally exhibit an acicular (e.g., needle-like) morphology that extend among one axis as
83 crystallization processes take place.²⁻⁴

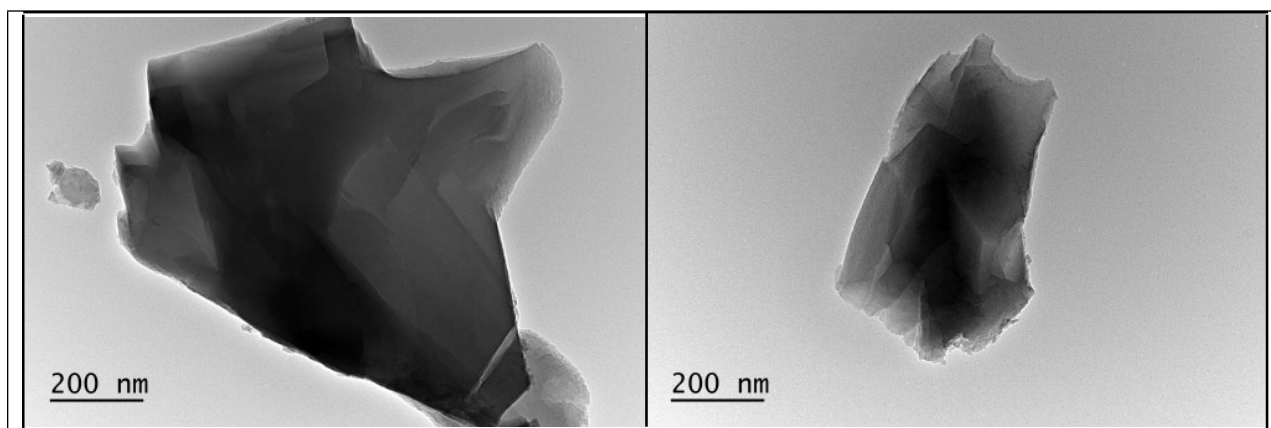


Figure S.7. TEM images of PHI-TOB-373-0.

84

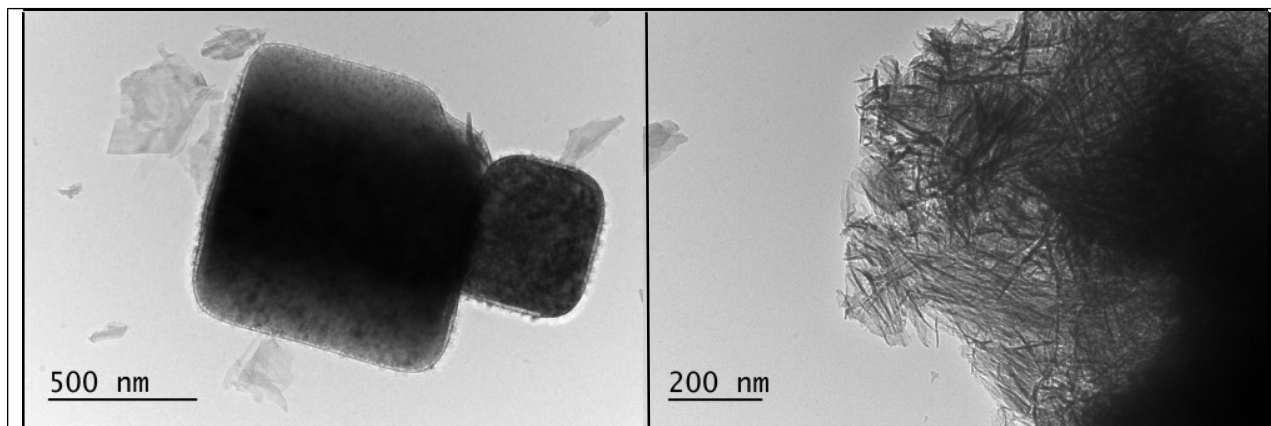


Figure S.8. TEM images of PHI-TOB-393-1.

85

86 **S.4. References.**

- 87 (1) Mumpton, F. A.; Ormsby, W. C. Morphology of Zeolites in Sedimentary Rocks by Scanning
88 Electron Microscopy. *Clays and Clay Minerals* **1976**, *24* (1), 1–23.
89 <https://doi.org/10.1346/CCMN.1976.0240101>.
- 90 (2) Diez-Garcia, M.; Gaitero, J. J.; Dolado, J. S.; Aymonier, C. Ultra-Fast Supercritical
91 Hydrothermal Synthesis of Tobermorite under Thermodynamically Metastable Conditions.
92 *Angewandte Chemie-International Edition* **2017**, *56* (12), 3162–3167.
93 <https://doi.org/10.1002/anie.201611858>.
- 94 (3) Huang, X.; Jiang, D.; Tan, S. Novel Hydrothermal Synthesis Method for Tobermorite Fibers
95 and Investigation on Their Thermal Stability. *Materials Research Bulletin* **2002**, *37* (11),
96 1885–1892. [https://doi.org/10.1016/S0025-5408\(02\)00854-1](https://doi.org/10.1016/S0025-5408(02)00854-1).
- 97 (4) Galvánková, L.; Másilko, J.; Solný, T.; Štěpánková, E. Tobermorite Synthesis Under
98 Hydrothermal Conditions. *Procedia Engineering* **2016**, *151*, 100–107.
99 <https://doi.org/10.1016/j.proeng.2016.07.394>.
- 100